J Electroceram (2006) 17:197–203
DOI 10.1007/s10832-006-0469-x

The electronic structures for the optical absorption of Hf-O-N thin films

Sung Kwan Kim · Yang-Soo Kim · Young-Ah Jeon · Jongwan Choi · Kwang-Soo No

Received: 29 June 2005 / Revised: 31 August 2006 / Accepted: 1 September 2006
© Springer Science + Business Media, LLC 2006

Abstract The local structures of Hf-O-N thin films were analyzed using an extended X-ray absorption fine structure (EXAFS) study on Hf L_{III}-edge and first-principles calculations. Depending on their composition and atomic configurations, Hf_4O_8 (CN: 7.0), $Hf_4O_5N_2$ (CN: 6.25) and $Hf_4O_2N_4$(CN: 5.5) were suggested as the local structures of Hf-O-N thin films. The optical band gaps of Hf-O-N thin films were compared with the calculated band gap. And to investigate the optical absorption, the effects of film compositions on the valence bands of Hf-O-N thin films were analyzed by comparing the experimental valence band with the valence band.

Keywords Hafnium oxynitride thin films · Electronic structures · Optical absorption

1 Introduction

Recently, HfO_2 and Hf-O-N thin films have attracted interest because of their unique properties, particularly their high dielectric constant, relatively large band gap, and stability. Given their high dielectric properties, these films have been investigated as a potential replacement of dielectric to reduce the tunneling current through the gate-oxide of a field-effect transistor (FET) [1–3]. In the lithographic process, Hf-O-N thin films have also been considered as a substitute for the phase-shift mask (PSM), because of their high refractive index. In deep ultraviolet (DUV) lithography, the phase-shift masks of Cr compounds and MoSiON have a low refractive index of less than 2.5. To satisfy the requirements of transmittance and phase shift, the thickness of Cr compounds and MoSiON should be greater than 90 nm [4]. This amount of thickness causes an error when patterns are formed on a wafer. An error can be reduced with the use of Hf-O-N thin films having a high refractive index.

The transmittance and the phase shift through the PSM depend on the optical constants (n: refractive index and k: extinction coefficient). It is important to investigate the optical absorption and electronic structures of the PSM, because the dispersions of optical constants are related to that [5]. In this study, we analyzed the electronic structures of Hf-O-N thin films using first-principles calculation to research the optical absorption of Hf-O-N thin films. Before we researched the electronic structures, the local structures of Hf-O-N thin films were analyzed using the extended X-ray absorption spectroscopy (EXAFS) and the structure optimization. Using the local structures, the electronic structures of Hf-O-N thin films such as the valence band and the optical band gap, were simulated. The effects of composition on the electronic structures and optical absorption of Hf-O-N thin films were analyzed.

2 Experimental methods

Hf-O-N thin films (50 ± 5 nm) (S1–S5) were deposited using a planar circular rf magnetron reactive sputtering system

S. K. Kim (✉) · J. Choi
SAMSUNG ELECTRONICS, Semiconductor Business San #24 Nongseo-Dong, Giheung-Gu, Yongin-City, Gyeonggi-Do, Korea 446-711

Y.-S. Kim
Sunchon Branch, Korea Basic Science Institute 315 Maegok, Sunchon, Jeonnam 540-742, Korea

Y.-A. Jeon · K.-S. No
Department of Materials Science and Engineering, Korea Advanced Institute of Science and Technology, Daejeon, 305-701, Korea
e-mail: ksgyon@kaist.ac.kr

with a 4" Hf target and a mixture of O_2 and N_2 gases (Ar: 20 sccm, O_2: 0, 1 sccm, N_2: 10, 20 sccm). The composition was determined by means of rutherford backscattering spectroscopy (RBS) and auger electron spectroscopy (AES). X-ray absorption spectra (XAS) measurements around Hf L_{III}-edge (9561 eV) were measured to investigate the local structures of Hf-O-N thin films at 7 C beam-line of the Pohang Accelerator Laboratory (PLS, Pohang, Korea). The optical properties of Hf-O-N thin films such as absorbance and optical band gap were estimated by UV spectroscopy (Hewlett Packard 8452A). The valence band spectra were measured using the 4B1 photoemission electron microscopy beam-line at the PLS [6].

In the structure optimization, first-principles calculations of total energies were carried out within the general gradient approximation (GGA)[7] of the density functional theory (DFT), using the *ab-initio* total-energy and molecular dynamics program VASP (Vienna *ab-initio* simulation package [8]. A plane-wave basis set combined with the projector augmented-wave method was employed [9]. A kinetic energy cutoff of 400 eV and a reciprocal-space k-point grid of dimensions $9 \times 9 \times 9$ were used. The unit cell including volume and shape and the atomic position were relaxed. The electronic structures were calculated using a program SCAT based on the discrete variational Xα (DV-Xα) method [10]. The cluster models for Hf-O-N thin films were designed using the local structures from extended X-ray absorption fine structure (EXAFS) analysis and the structure optimization. Each cluster model is embedded in point charges located at the external atomic sites so as to produce an effective Madelung potential.

3 Results and discussion

3.1 The local structures of Hf-O-N thin films

In the previous research [11], the local structures of Hf-O-N thin films were analyzed using a curve-fitting analysis of the filtered back-transformed EXAFS spectra and first-principles calculations (Table 1). From EXAFS analysis, it was confirmed that the coordination number (CN) in the first-shell decreased from 6.95 to 5.11 as the N/Hf ratio increased, and that the bond length in the first-shell of S1, S2 and S3 slightly decreased from 2.179 to 2.154 Å as the N/Hf ratio increased. The increase of film density was considered as one of the cause about the decrease of the bond length [12]. However, the bond length of S4 and S4 increased abruptly to 2.194 Å and 2.187 Å. Considering the composition of S4 and S5, S4 and S5 were expected to have the structure of Hf_2ON_2 with the bond length of 2.17 Å when they were crystallized [13].

Considering the film composition and the coordination number (CN) around Hf ions, $Hf_4O_5N_2$ (CN: 6.25) with $(1V_O^{1st} + 2O_N)$ and $Hf_4O_5N_2$ (CN: 6) with $(1V_O^{2nd} + 2O_N)$ were suggested as the local structures for S3. And the local structures of $Hf_4O_2N_4$(CN: 5.5) derived by forming $(2V_O^{1st} + 4O_N)$, $Hf_4O_2N_4$(CN: 5.25) by $(1V_O^{1st} + 1V_O^{2nd} + 4O_N)$, and $Hf_4O_2N_4$(CN: 5.0) by $(2V_O^{2nd} + 4O_N)$ were suggested as the local structures for S5 (Fig. 1). The term V_O refers to the vacancy of O ions, and the term O_N indicates that O ion is substituted by N ion. All local structures with the different combination were optimized geometrically, and the local structure having the minimum total energy was selected. By comparing the bond length for the first-shell from EXAFS analysis and the average bond length for local structures from the structure optimization, Hf_4O_8 (CN: 7.0) for S1, $Hf_4O_5N_2$ (CN: 6.25) for S3 and $Hf_4O_2N_4$ (CN: 5.5), $Hf_4O_2N_4$ (CN: 5.0) for S5 were selected.

3.2 The electronics structures for the optical absorption spectra of Hf-O-N thin films

Figure 2(a) shows the $(\alpha h\nu)^{0.5}$ as a function of the photon energy $h\nu$ for all samples. According to Tauc's formula [14],

$$(\alpha h\nu)^{1/2} = const.\,(h\nu - E_g)(\alpha : \text{absorption coefficient, } \hbar\omega : \text{photon energy}) \quad (3)$$

$$\alpha = 2.303 \times \frac{\log(I_0/I)}{d}\ (\mathrm{cm}^{-1})\,(\alpha : \text{absorption coefficient, } \log(I_0/I) : \text{absorbance, } d : \text{film thickness}) \quad (4)$$

The curves present a linear part for high values of $(\alpha h\nu)^{0.5}$, attributed to optical transitions between extended states in the parabolic range of the density of states. The extrapolation of this linear part to zero yields the optical band gap (Fig. 2(b)). The optical band gap calculated using Tauc's rule is changed from 4.1 to 1.98 eV with a function of the N/Hf ratio. Similar results of a decreasing band gap have been observed for metal oxynitrides as well [12].

In the comparison of the optical band gap and the calculated band gap, the optical band gap of S1 (4.3 eV) differs from the simulated band gap (3.69 eV) of Hf_4O_8 (CN: 7.0). It can be due to the inherent errors in DFT band gaps that the band gaps calculated within local density approximation (LDA)/GGA are always underestimated compared to experiments. The crystallized m-HfO_2 thin film with thickness of 900 nm has the optical band gap of 4.7 eV that is higher than the calculated band gap (3.9 eV) of bulk m-HfO_2. Considering the error between experimental and calculated band gap (0.8 eV), the difference (1.1 eV) of band gap for S3 is critical. $Hf_4O_2N_4$ (CN: 5.5) is selected as the local structure for

Table 1 The local structures from EXAFS analysis (a) and from the structure optimization using first-principles calculations (b) for Hf-O-N thin films

Sample number	Local structures by EXAFS analysis (a) CN	Inter-atomic distance for the first-shell (Å)	Local structures by the structure optimization (b) Models	CN	Atomic configuration	Average bond length(R^{ave}) for Hf−O/N bonds (Å)
m-HfO_2	3	2.139	Hf_4O_8	7.0	No defects	2.139 (0.03)
	4	2.259				
S1	2.99	2.108				
	3.96	2.234				
S2	2.99	2.097	$Hf_4O_5N_2$	6.25	$1V_O^{1st} + 2O_N$	2.129 (0.013)
	3.89	2.223		6.0	$1V_O^{2nd} + 2O_N$	2.115 (0.024)
S3	2.85	2.088				
	3.57	2.207				
S4	2.45	2.127	$Hf_4O_2N_4$	5.5	$2V_O^{1st} + 4O_N$	2.163 (0.010)
	3.31	2.244		5.25	$1V_O^{1st} + 1V_O^{2nd} + 4O_N$	2.130 (0.014)
S5	2.28	2.120		5.0	$2V_O^{2nd} + 4O_N$	2.165 (0.014)
	2.83	2.241				

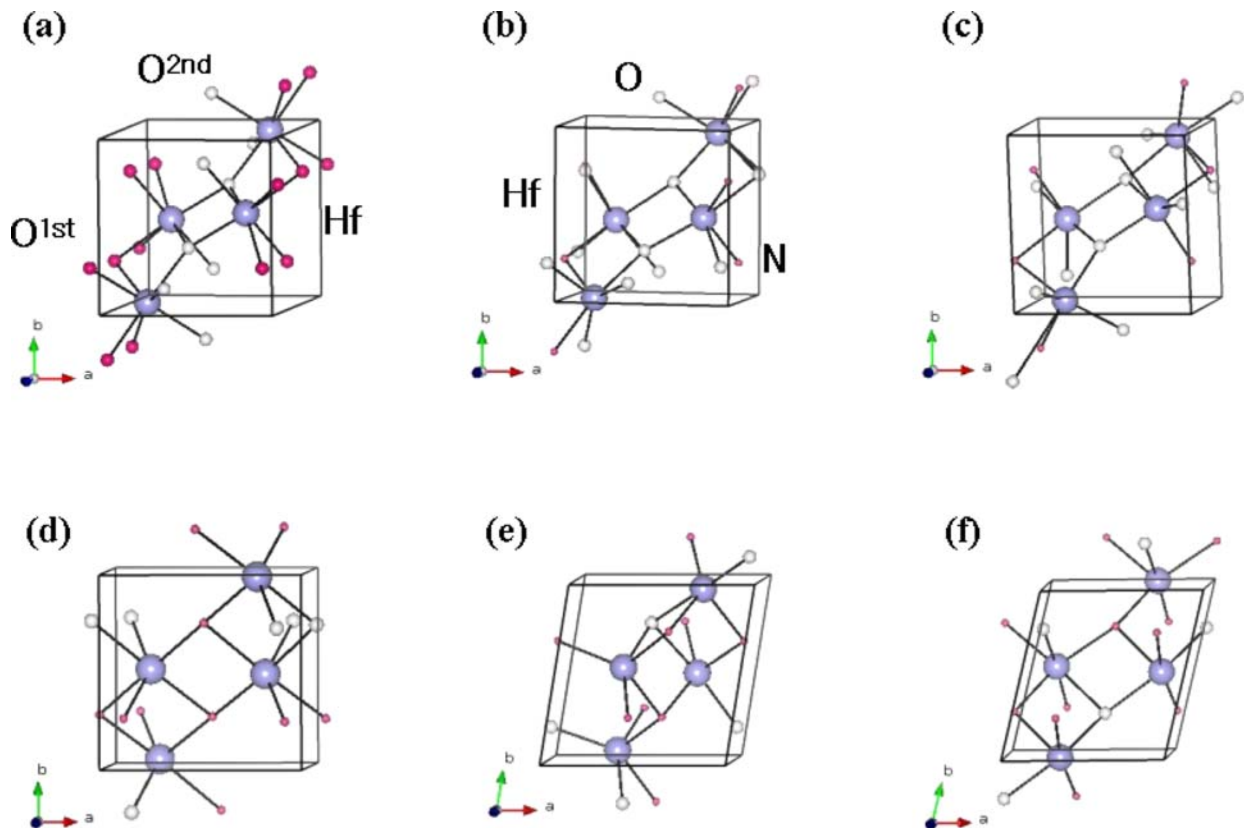

Fig. 1 The local structures for Hf-O-N thin films. HfO_2 (a) (CN: 7.0) for S1 (large gray balls: Hf, medium light balls: O^{1st} and medium dark ball: O^{2nd}), two local structures of $Hf_4O_5N_2$ (CN: 6.25) (b) and $Hf_4O_5N_2$ (CN: 6.0) (c) for S3, three local structures of $Hf_4O_2N_4$ (CN: 5.5) (d), $Hf_4O_2N_4$ (CN: 5.25) (e) and $Hf_4O_2N_4$ (CN: 5.0) (f) for S5. (large gray balls: Hf, medium light balls: O and small dark ball: N)

S5 because the simulated band gap of $Hf_4O_2N_4$ (CN: 5.0) is higher than the optical band gap of S5.

To verify the effects of film compositions on the optical absorption, the valence band spectra of Hf-O-N thin films that were recorded using 220 eV of the photon energy (Fig. 3). The O/Hf and N/Hf ratio of Hf-O-N thin films were 1.71 (± 0.04) and 0.08 (± 0.02) for S1, 1.36 (± 0.04) and 0.38 (± 0.07) for S3, and 0.20 (± 0.15) and 1.1 (±

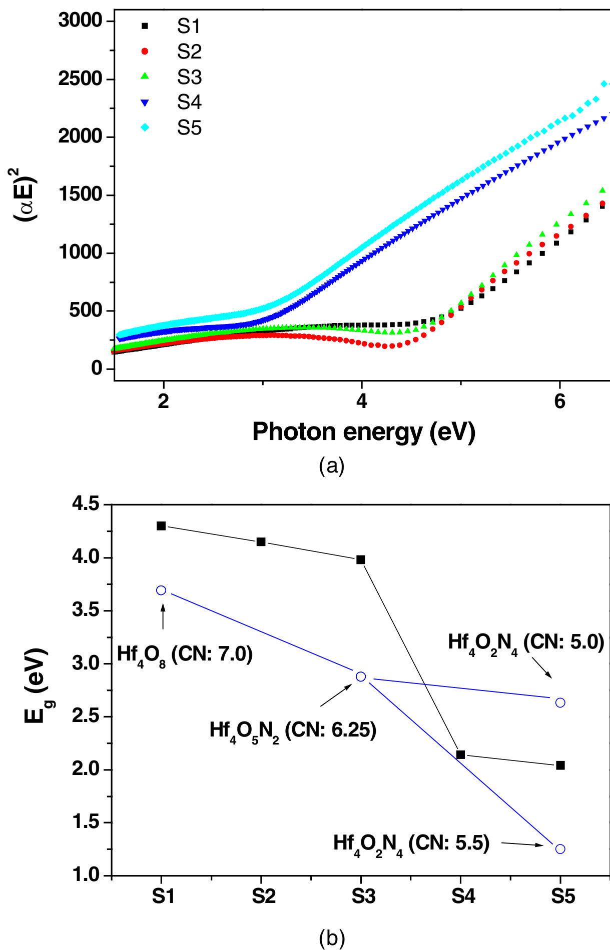

Fig. 2 The $(\alpha h\nu)^{0.5}$ variation (a) and the optical band gap variation (b) of Hf-O-N thin films

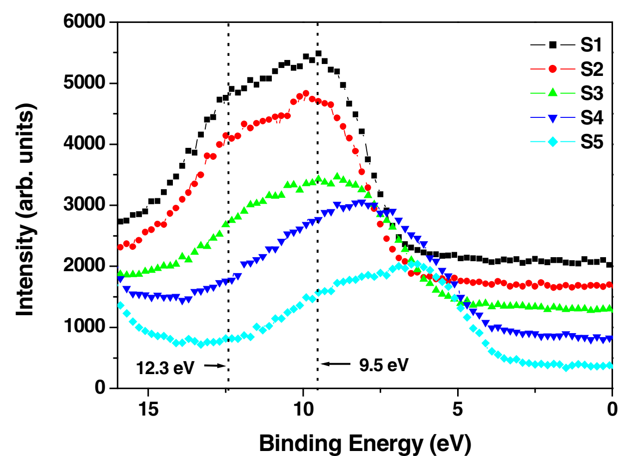

Fig. 3 The valence band spectra of Hf-O-N thin films. The spectra were recorded using 220 eV of the photon energy

0.1) for S5. As the N/Hf ratio increases, the valence band shifts to a low binding energy and the gap between the valence band and Fermi energy level decreases. The shift of the valence band to a low binding energy is considered as one of reasons about the decrease of optical band gaps.

The valence bands of S1, S3 and S5 were compared the calculated valence bands of Hf_4O_8 (CN: 7.0) for S1, $Hf_4O_5N_2$ (CN: 6.25) for S3 and $Hf_4O_2N_4$ (CN: 5.5), $Hf_4O_2N_4$ (CN: 5.5) for S5 (Fig. 4). All density of states were shifted to fix the Fermi energy to 0 eV. For S1 (Fig. 4(a)), the valence band is mainly composed of three peaks at −1.9 eV, −5.1 and −7.0 eV that all peaks are related to the bonding interaction of Hf 5d–O 2p bonds. The peak at −1.9 eV is related to the anti-bonding interaction between Hf 5d–Hf 5d and two peaks at −5.1 eV, −7.0 eV are related to the bonding interaction of Hf 5d - Hf 5d. The optical absorption was due to the electron transition from O 2p in the valence band and Hf 5d in the conduction band [15].

The valence band of $Hf_4O_5N_2$ (CN: 6.25) in the range from –12.5 eV to the valence band edge contains several peaks (Fig. 4(b)). These peaks are classified into three parts as kinds of bonds that contribute to peaks. The weak peak at over –1.0 eV is manly related to the bonding interaction of Hf 5d−N 2p. Peaks from –1.0 to –10.0 eV are due to the bonding interaction of Hf 5d–O 2p and Hf 5d–N 2p even though the contribution by Hf 5d–O 2p bonds is larger than that by Hf 5d–N 2p. Peaks at below −9.8 eV are related to the bonding interaction of Hf 5d–O 2p.

In the indirect absorption, the transition rate is expressed as the multiplication of the density of states in the valence band and the conduction band, and the absorption coefficient is related to the transition rate [16]:

$$W_{ca} \propto |V^{\omega_k}|^2\,|V^{\omega}|^2 \int_0^{\hbar\omega+\hbar\omega_k-E_G} \rho_v(E-\hbar\omega-\hbar\omega_k)\rho_c(E)dE \tag{4}$$

$$\alpha_{ji} = \varepsilon_1 W_{ji}/nc \tag{5}$$

(The probability of the photon absorption ($|V^{\omega}|^2$) is nearly constant for a direct transitions are allowed. W is the transition rate and α is the absorption coefficient).

It indicates that the absorption coefficient for a direct transition to energy E from an initial energy E-$h\omega$ is proportional to the product of the initial density of states and the final density of states. When S3 absorbs a light having photon energy over band gap, electrons in N 2p in the valence band are excited to Hf 5d related to Hf−N bonds in the conduction band. It is speculated that the increase of the absorption coefficient is low because the pDOS of Hf 5d and N 2p related to Hf−N bonds is small. When a photon with the higher photon energy is absorbed, it is expected that the absorption coefficient increase abruptly because the pDOS of Hf 5d and N 2p related

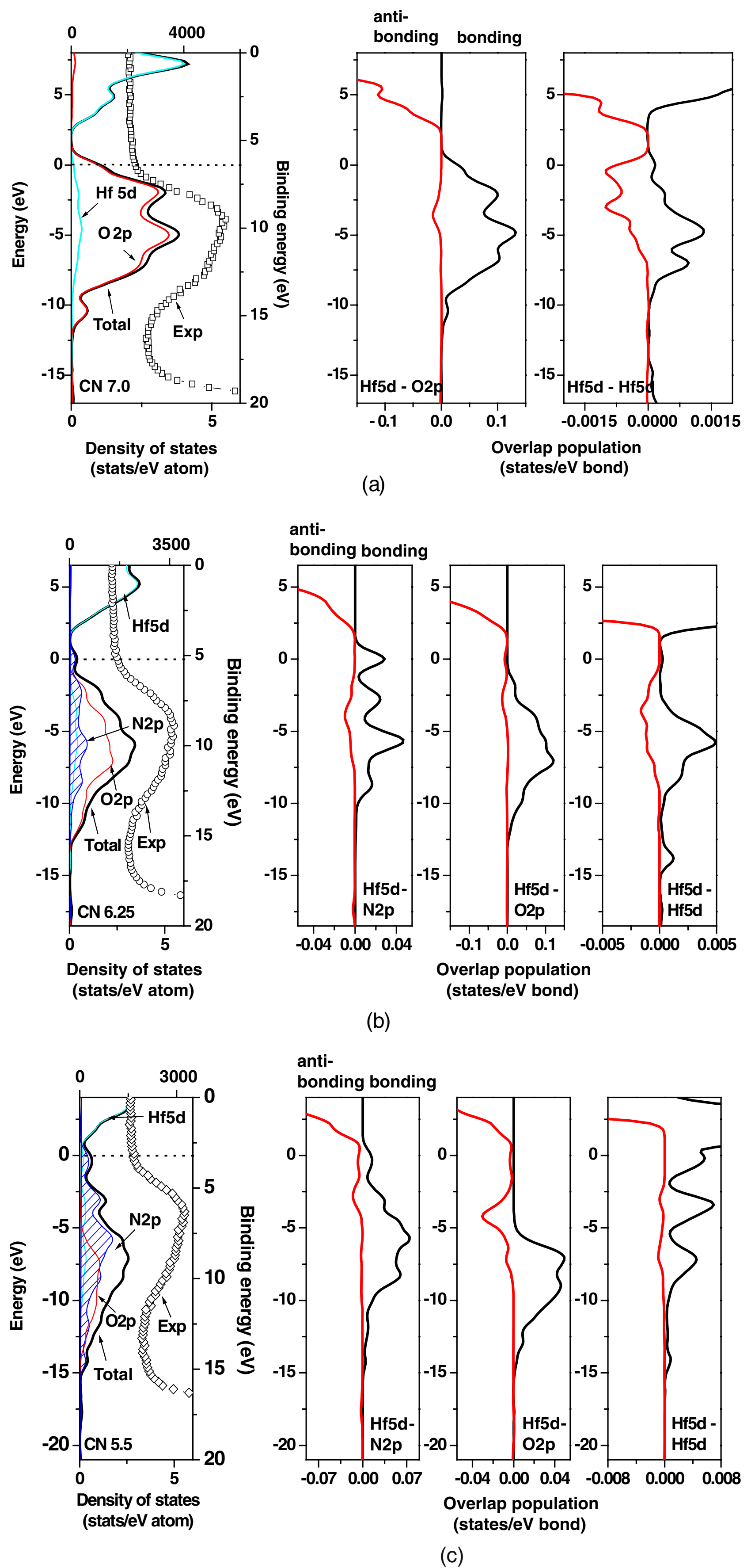

Fig. 4 Density of states for the valence bands, the bond-overlap populations of Hf–O bonds, Hf–N bonds and Hf–Hf bonds for Hf_4O_8 (CN: 7.0) (a), $Hf_4O_5N_2$ (CN: 6.25) (b), $Hf_4O_2N_4$ (CN: 5.5) (c)

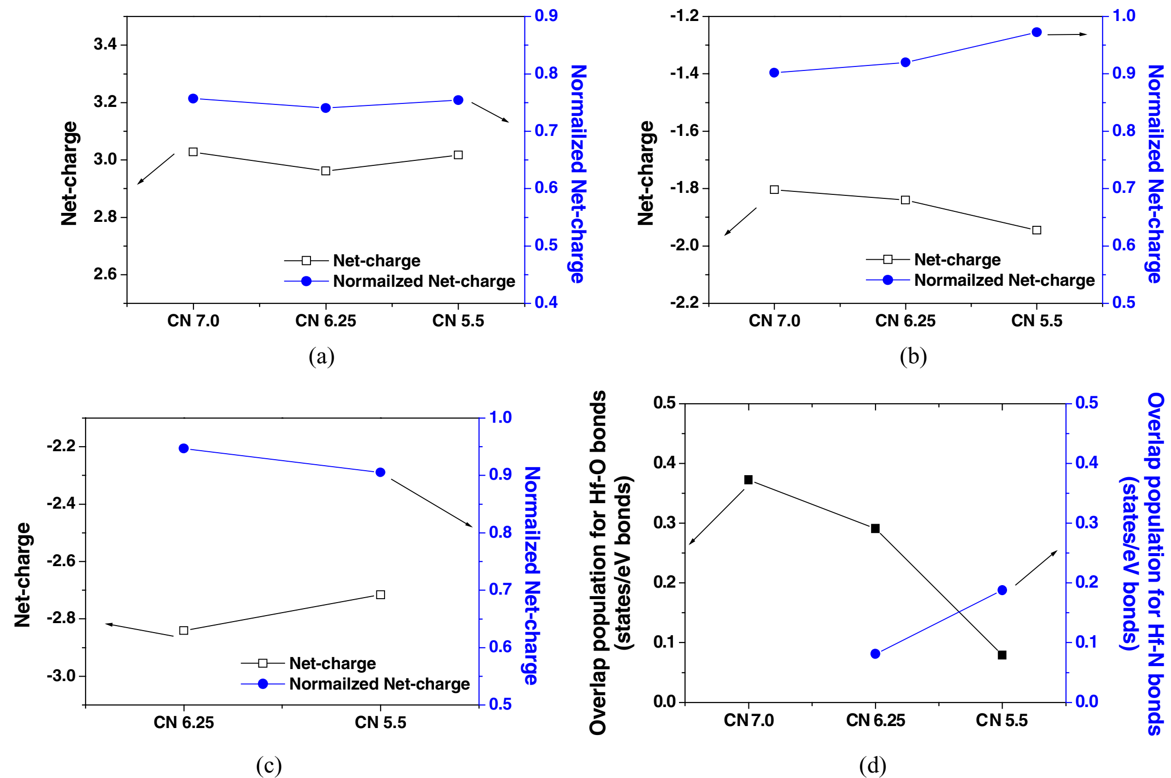

Fig. 5 The net-charge and the normalized net-charge of Hf ions (a), O ions (b) and N ions (c), and the overlap population (d) of the Hf–O bonds and the Hf–N bonds for Hf_4O_8 (CN: 7.0), $Hf_4O_5N_2$ (CN: 6.25), $Hf_4O_2N_4$ model (CN: 5.5)

to Hf−N bonds is large. The low transition rate and absorption coefficient for the electron transition from N 2p to Hf 5d is considered as one of the reasons for the difference between the optical band gap (3.98 eV) and the simulated band gap (2.88 eV).

Similar results for $Hf_4O_2N_4$(CN: 5.5) are obtained (Fig. 4(c)). Peaks at over −5.0 eV are contributed by the bonding interaction of Hf 5d and N 2p. Peaks at from –5.0 to–10.0 eV are due to the bonding interaction of Hf 5d–O 2p and Hf 5d–N 2p. Peaks at below –10.0 eV are related to the bonding interaction of Hf 5d–O 2p. The part related to Hf 5d–N 2p in $Hf_4O_2N_4$ (CN: 5.5) is stronger than that in $Hf_4O_5N_2$(CN: 6.25) because of the high N/Hf ration. It is expected that when S5 absorbs a light having photon energy over band gap, the absorption coefficient increases abruptly because the pDOS of Hf 5d and N 2p related to Hf−N bonds is large.

Figure 5 shows the net-charge of Hf, O, and N ions ((a), (b) and (c)) and the bond overlap population of Hf–O bonds and Hf–N bonds ((d)). The net-charge of each ion is normalized by the formal charge of −4 for Hf, −2 for O and −3 for N. When the normalized net-charge is closer to 1, the ionic bonding character is stronger. The normalized net-charge of Hf ion is constant regardless of film composition. It is related to that the absorption edge of X-ray absorption spectra for Hf L_{III}-edge was constant regardless of film composition in the previous research. The normalized net-charge of O ion increases as the N/Hf ratio increases. It is related to the decrease of the bond overlap populations for Hf-O bonds. And the decrease of the normalized net-charge for N ions is also related to the increase of the bond overlap populations for Hf–N bonds. These results indicate that the ionic bonding character of the Hf−O bonds and the covalent bonding character of the Hf-N bonds in $Hf_4O_2N_4$ (CN: 5.5) are stronger than that in $Hf_4O_5N_2$ (CN: 6.25) are. The stronger covalent bonding character of the Hf-N bonds is related to the narrower band gap of Hf−O−N thin films because the highest occupied molecular orbital (HOMO) and the lowest unoccupied molecular orbital (LUMO) energy levels are formed by the hybridization of Hf 5d and 2 N 2p.

4 Conclusion

Using the suggested local structures of Hf_4O_8 (CN: 7.0), $Hf_4O_5N_2$ (CN: 6.25) and $Hf_4O_2N_4$ (CN: 5.5) in the previous research, we analyzed the effects of composition on the optical band gaps and valence band spectra of Hf-O-N thin films. The optical band gaps of S1 and S5 are consistent with the simulated band gap of Hf_4O_8 (CN: 7.0) and $Hf_4O_2N_4$ (CN: 5.5) in error e while the difference

between the optical and simulated band gap of S3 is critical.

The valence band spectra of Hf-O-N thin films were analyzed by comparing it with the bond overlap population diagrams for Hf_4O_8 (CN: 7.0), $Hf_4O_5N_2$ (CN: 6.25) and $Hf_4O_2N_4$ (CN: 5.5). The N 2p forms the HOMO between the valence and conduction bands of HfO_2 via hybridization of the N 2p and the Hf 5d. Thus, the valence band shifts to the low binding energy and the band gap decreases as the N/Hf ratio increases. Based on the electronic structure for the valence band of S3, the transition rates for the direct transition is suggested as one of reasons for the difference between the optical and simulated band gap. Based on the chemical bonding characteristics for Hf−O bonds and Hf−N bonds, it was confirmed that the stronger covalent bonding character of the Hf−N bonds is related to the narrower band gap of Hf-O-N thin films.

Acknowledgments This work was supported by the Ministry of Education (“Brain Korea 21”) and the Ministry of Science and Technology (MOST), Korea. The experiments at the Pohang Accelerator Laboratory were supported in part by MOST and Pohang Iron and Steel (POSCO). Special thanks Isao Tanaka for supporting the *ab initio* total-energy and molecular dynamics program VASP (Vienna *ab initio* simulation package).

References

1. *The National Technology Roadmap for Semiconductors* (Semiconductor Industry Association, Sematech, Austin, 2000).
2. J. Kang, E.-C. Lee, and K.J. Chang, *Phys. Rev.* B, **68**, 054106 (2003).
3. G.-M. Rignanese, X. Gonze, G. Jun, K. Cho, and A. Pasquarello, *Phys. Rev.* B, **69**, 184301 (2004).
4. S.K. Kim, M.A. Kang, J.M. Shon, S.H. Kim, and K. No, *Opt. Mater.*, **22**, 361 (2003).
5. X. Rocquefelte, F. Goubin, H.J. Koo, M.H. Whangbo, and S. Jobic, *Inorg. Chem.*, **43**, 2246 (2004).
6. T.H. Kang, K. Kim, C.C. Hwang, S. Rah, C.Y. Park, and B. Kim, *Nucl. Instrum. Methods Phys. Res.* A, **467**, 581 (2001).
7. Y. Wang and J.P. Perdew, *Phys. Rev.* B, **44**(13), 928 (1991).
8. G. Kresse and J. Furthmüller, *Phys. Rev.* B, **54**(11), 169 (1996).
9. D. Vanderbilt, *Phys. Rev. B*, **41**, 7892 (1990).
10. H. Adachi, M. Tsukada, and C. Satoko, *J. Phys. Soc. Japan*, **45**, 875 (1978).
11. S.K. Kim, Y.S. Kim, and K.S. No, X-ray spectrometry (in press).
12. S. Venkataraj, D. Severin, S.H. Mohanmed, J. Ngaruiya, O. Kappertz, and M. Wutting, Thin Solid Films (in press).
13. S.J. Clarke, C.W. Michi, and M.J. Rosseinsky, *J. Solid State Chem.*, **146**, 399 (1999).
14. J. Tauc, R. Grigorovichi, and A. Vancu, *Phys. Status Solidi.*, **15**, 527 (1996).
15. S.K. Kim, Y.S. Kim, J.I. Hong, I. Tanaka, and K. No, *J. App. Phys.*, **97**, 073519 (2005).
16. F. Wooten, *Optical Properties of Solids* (Academic Press, Inc. 1972), Chap. 5.